

RELATIVE PERMEABILITY ANALYSIS FOR GRAVITY DRAINAGE OF VISCOUS OILS

David Element, Stephen Goodyear, Jacqui Green, Jane Johnston and Nicola Sargent

AEA Technology, Winfrith, Dorchester, Dorset DT2 8DH, UK

Presented at the IEA Collaborative Project on Enhanced Oil Recovery
19th International Workshop and Symposium, Carmel, California, October 1998

ABSTRACT

Gas injection into a primary gas cap, where this exists, may provide an alternative strategy to water flooding for viscous oil fields, giving lower effective residual oil saturations (because of the much greater density contrast between oil and gas compared to that between water and oil). A knowledge of the expected character of gravity drainage gas/oil relative permeabilities in high permeability, unconsolidated formations is required to assess the potential benefits from gas injection compared to water flooding.

Measurements of gas/oil relative permeabilities are typically made under viscous dominated flooding conditions, which are unrepresentative of gravity drainage conditions in the field, and without the benefit of in-situ saturation monitoring which is essential to remove laboratory artefacts arising from capillary end effects. To address these issues we performed a series of gas/oil gravity drainage experiments in high permeability sandpacks using oil viscosities of 2 cp, 23 cp and 208 cp. Oil drainage was measured using in-situ saturation monitoring.

Analysis of pressure drop data during core conditioning, allowed regions of low oil permeability at the inlet and outlet ends of the sandpacks to be excluded from the subsequent analysis and gave a local value of permeability for the central region of the packs. Use of total pressure drop data alone to determine the average permeability would have underestimated the permeability of the central region of the pack by a factor of 4-5, as a consequence the relative permeabilities would have been too high by the same factor.

Oil relative permeabilities have been calculated from the in-situ saturation data for the three sandpacks. The relative permeabilities lie on the same curve, showing that oil relative permeabilities are independent of viscosity over the range 2 to 200 cp in these sandpacks.

Comparison of the sandpack relative permeabilities with data previously obtained from consolidated Clashach sandstone, shows that the relative permeabilities in the sandpacks are approximately a factor of 300 higher over the saturation range considered. Gravity drainage in high permeability unconsolidated reservoirs, even with viscous oils, is therefore potentially a very efficient displacement technique.

One dimensional solutions for vertical displacement of oil by gas have been constructed and the effective residual oil saturation at breakthrough determined for a wide range of viscosities (1 cp to 1000 cp) and frontal advance rates (including typical reservoir rates) for vertical permeabilities of 1000 and 5000 md. Under appropriate conditions, effective residual oil saturations of ~10% may be obtained for oils of 100 cp.

INTRODUCTION

Gas injection into a primary gas cap, where this exists, may provide an alternative strategy to water flooding for UKCS high permeability viscous oil fields, giving lower effective residual oil saturations (because of the much greater density contrast between oil and gas compared to that between water and oil). A knowledge of the expected character of gravity drainage gas/oil relative permeabilities in high permeability, unconsolidated formations is required to assess the potential benefits from gas injection compared to water flooding.

Measurements of gas/oil relative permeabilities are typically made under viscous dominated flooding conditions, which are unrepresentative of gravity drainage conditions in the field, and without the benefit of in-situ saturation monitoring which is essential to remove laboratory artefacts arising from capillary end effects.

To address these issues, a series of gas/oil gravity drainage experiments in high permeability sandpicks using oil viscosities of 2 cp, 23 cp and 208 cp have been performed, with the drainage of oil in the packs measured using in-situ saturation monitoring.

The time evolution of the in-situ saturation data was used to deduce oil relative permeabilities under gas gravity drainage. These were compared for different oil viscosities and with results from floods in consolidated core obtained in previous studies. The effective residual oil saturation at reservoir flow rates was calculated for a range of permeabilities and viscosities covering typical UKCS viscous oil fields.

LABORATORY PROCEDURES

Preparation of Sandpicks

Three sandpicks were constructed using glass columns 2.5 cm in diameter, with pick lengths of approximately 70 cm. Fine PTFE filters separate the sand from the end caps to prevent sand grains entering the fluid lines. The sand was selected to give pick permeabilities of approximately 5 Darcy at 100% brine saturation, representative of UKCS viscous oil fields.

As the in-situ monitoring system requires 100% gas calibration, the column was dry-packed. Uniform packing was achieved by continually pouring sand into the top of the column via a funnel whilst tapping the column at the point where the sand was settling with a rubber spatula to allow the grains to settle evenly.

Fluids

Chesil sea water was selected as the brine phase. Kathon biocide was added to the brine at 5 ppm as the flood duration extended over several months. The brine was filtered to 0.45 μ m and degassed by helium sparging before use.

Castrol's Magna lubricating oils were selected for the experiments due to their purity and wide viscosity range. The oil compositions used in the floods are given in Table 1. The Magna oils are highly refined straight mineral oils. Iodododecane was used to increase the

γ -attenuation of the oil phase and optimise phase analysis. Exposure of the doped oils to light was minimised since iodododecane is photosensitive [1]. Attenuation scans were conducted on doped oil samples throughout the experiments in order to assess any degradation with time.

Table 1. Composition and Characteristics of Test Oils

Sandpack	Ratio of component			Viscosity at 22°C	Density at 22°C
	Magna 320	Magna 2	Iodododecane	(cp)	(g/cc)
1	4	-	1	208	0.944
2	-	4	1	2.7	0.877
3	2.4	1.6	1	23.5	0.917

The gas used in the experiments was nitrogen.

The spreading behaviour of the oils on brine was determined by placing a drop of oil on the surface of the brine in the presence of air and monitoring the rate at which the drop diameter increased. All the oils spread over the surface of the brine immediately on contact, with final thicknesses of the film of 52.0 μm , 25.5 μm and 16.6 μm for the 2.7 cp, 23.5 cp and 208 cp oil respectively.

Measurement of In-situ Saturations

The fluid saturations in the sandpacks were monitored during floods by gamma attenuation, using collimated Americium-241 sources and CsI scintillation detectors.

The gamma-attenuation method can only be used to measure two phases. However, it can be used in three phase floods, provided one of the phases is immobile. This requires calibrations for the sandpack for 100% saturations of the fluids to be used in the experiment. No water was produced during the gas injection phase of the floods and agreement between effluent and in-situ mass balances was good. 100% gas calibrations were obtained for the dry sandpacks and 100% water calibrations when the sandpacks had been vacuum saturated with degassed brine. The 100% oil calibrations were measured at the end of the gas floods. The sandpacks were solvent cleaned with toluene and methanol before flooding to 100% oil saturation with the same oil as had been used in the gas injection experiment.

The movement of the source/detector assembly and the collection of the counts was computer controlled, enabling automated scanning. The columns were scanned at 0.5 cm intervals along the complete length of the column. At the end of each scan a datum reference reading was taken on an aluminium bar positioned below the sandpacks. The datum counts were compared with an average reading taken on the bar at the start of the experiments so that a correction factor could be calculated to account for any changes in the characteristics of the electronics. Individual data points were then corrected by this factor.

The rig was contained in an air conditioned laboratory maintained at a nominal temperature of $22\pm 0.5^{\circ}\text{C}$.

Pressure Measurements

Pressure readings were taken from transducers situated outside the end caps. Permeability measurements and compressibility tests were conducted at each stage of the experiment prior to proceeding.

CORE FLOODING SEQUENCE

Flood to Connate Water

Once the 100% brine calibrations had been obtained, all the sandpacks were flooded to connate brine with the 208 cp oil (doped with 20% iodododecane). The same oil was used for all the sandpacks to enable a direct comparison to be made between the experiments without large differences in the magnitude of the connate brine saturations. Fluids were recirculated via a volume separator so that a mass balance determination of connate brine saturation could be made. The floods were stopped when there was no further brine production in the recirculating reservoir, the oil distribution (as indicated via attenuation scans) was constant, and reproducible permeabilities had been established.

Ageing with Stock Tank Oil

At the end of the connate water flood the heavy oil was displaced with kerosene and the kerosene was then displaced with stock tank crude oil. The kerosene was used as a buffer to avoid potential asphaltene deposition on mixing heavy oil directly with stock tank oil. The core was aged for a period of 20 days. At the end of the ageing period the stock tank oil was displaced by kerosene and the kerosene was then displaced with the doped refined oil until the attenuation scans were constant.

Gravity Stable Gas Flood

The flow circuit used for the secondary nitrogen injection is illustrated in Figure 1. Nitrogen was supplied to the top of the sandpack via a partially filled brine column which saturated the gas phase with water vapour. The gas bottle regulator was set to approximately 4 bar for each sandpack.

The outlet of the sandpack was connected to a calibrated separator which was initially filled with demineralised water. During the course of the experiment water was extracted from the bottom of the separator at a constant rate whilst produced fluids entered the top of the separator. The fluids were extracted at a nominal rate of 0.2 ml/hr from Sandpacks 1 and 3 and 2 ml/hr from Sandpack 2. The volumes of the produced phases were measured by monitoring the levels of the phase interfaces in the separator.

Flood to 100% Oil

At the end of the gas floods the sandpacks were solvent cleaned with toluene and methanol. The toluene was then miscibly displaced with the doped oil which had been used in each respective sandpack. The sandpacks were scanned whilst being flooded with oil.

Once the counts obtained were constant and a compressibility check confirmed that negligible volumes of gas remained, 100% oil calibration scans were obtained.

RESULTS

2.7 cp oil (Sandpack 2)

Fluid was extracted from the core at a higher rate of 2.0 ml/h during gas injection. This was to increase the amount of drainage observed behind the gas front to allow relative permeabilities to be calculated over a meaningful range of saturations. Gas breakthrough occurred at 0.75 PV. A selection of in-situ saturation profiles are shown in Figure 2. The spatial distribution of the initial brine saturation, prior to the gas injection, is reasonably constant across the centre of the sandpack, with a core average value of 12.4 % (by material balance). Following gas injection, the profiles show high oil saturations near the inlet throughout the gas flood (thought to be an artefact associated with the injection of the stock oil) and some hold-up of oil near the outlet as a result of a capillary pressure end effect. The displacement is very efficient, with very little evidence of local hold-up of oil at the end of the flood.

23.5 cp oil (Sandpack 3)

Fluid was extracted from the core at a rate of 0.19 ml/h during gas injection. Gas breakthrough occurred at 0.71 PV. A selection of in-situ saturation profiles are shown in Figure 3. The spatial distribution of the initial brine saturation, prior to the gas injection, is reasonably constant across the centre of the sandpack, with a core average value of 11.1% (by material balance). Following gas injection, as in Sandpack 2, the profiles show high oil saturations near the inlet and some evidence for a capillary pressure end effect. The displacement is efficient, with little evidence of local hold-up of oil.

208 cp oil (Sandpack 1)

Fluid was extracted from the core at a rate of 0.2 ml/h during gas injection. Gas breakthrough occurred at 0.34 PV. A selection of in-situ saturation profiles are shown in Figure 4. The spatial distribution of the initial brine saturation, prior to the gas injection, is reasonably constant across the centre of the sandpack, with a core average value of 8.8% (by material balance). Following gas injection, as in Sandpacks 2 and 3, the profiles show an inlet artefact and some evidence for a capillary pressure end effect. Early in the flood the saturation profiles in the central regions of the core show significant local variations in saturation, although at later times these become less pronounced as oil continues to drain under the action of gravity.

ANALYSIS OF IN-SITU SATURATION DATA FOR RELATIVE PERMEABILITIES

Theoretical Basis for Analysis Technique

The relative permeability can be computed from saturation measurements in a gravity stable experiment using the equation [2]:

$$k_{ro}(z, t) = -\frac{\mu_o}{K(\rho_o - \rho_g)g} \frac{\partial}{\partial t} \int_0^z \phi S_o dz, \quad (1)$$

which assumes that capillary pressure can be neglected and that viscous pressure drops are small compared with gravity head terms. Solving equation (1) requires some smoothing of the measured data. Reference [2] presents a variety of different smoothing methods. In this study, *variable time point t^b (Buckley-Leverett) smoothing* has been employed, although all relative permeability calculations have been checked using the *variable time point e^{-bt} (exponential) smoothing*.

The gas floods analysed here included a significant number of measurements of saturation prior to the gas front passing the various measurement depth stations. The procedure for computing relative permeabilities ensures that no relative permeability is evaluated unless the gas front has passed the depth station of interest and the particular saturation measurement has sufficient time-neighbours to allow accurate smoothing with no extrapolation of data.

Permeability Distribution

The calculation of relative permeabilities from the in-situ saturation data requires a knowledge of the permeability. Previous studies had suggested that the permeability could be different at the ends of the pack as a result of the packing procedure and the injection of stock tank oil. The pressure drop was monitored in each sandpack during the flood to connate water (displacing brine with 208 cp oil) and also when displacing kerosene with the Magna oils. By considering this as a piston-like displacement, the local permeability at the oil front is readily determined from the rate at which pressure drop per unit flow rate increases with total injected fluid according to:

$$\frac{d(\Delta p / Q)}{dW} = \frac{1}{\phi \Delta SA^2} \left(\frac{\mu_D}{k_D(W / (\phi \Delta SA))} - \frac{\mu_i}{k_i(W / (\phi \Delta SA))} \right), \quad (2)$$

where $k_D(x)$ and $k_i(x)$ are the permeabilities to the displacing and in-place fluid respectively, as a function of distance from the inlet of the core.

Although in-situ permeability values were derived from the flood-to-connate pressure data collected for Sandpacks 1 and 2, the noise in the pressure data meant that useful permeability data could only be derived by relatively coarse spatial-averaging, so it did not prove possible to determine the local permeability sufficiently accurately to allow correlation with the local porosity. However, it did allow the low-permeability regions at the end of the packs to be excluded from the evaluation of average permeability, Table 2.

Table 2: Summary of Brine Permeability Data

	Central region permeabilities from viscous oil floods		Pack average permeabilities from total pressure drop	
	Before Ageing (Darcy)	After Ageing (md)	Before Ageing (Darcy)	After Ageing (md)
Sandpack 1	3.85	800	3.0	270
Sandpack 2	4.00	-	2.6	150
Sandpack 3	no data available	1000	2.02	190

The permeability after ageing can be estimated from pressure changes during the viscous flood to displace kerosene with the Magna oils to be used in the gravity drainage measurements. As Table 2 shows, the effect of ageing with crude oil is to reduce the permeability in the central region of each sandpack by a factor of approximately 4-5. The 2 cp Magna oil employed in Sandpack 2 had a similar viscosity to the kerosene (measured as 1.1 cp), so the displacement of kerosene would not have been piston-like in that pack.

Based on the analysis of permeability in the central region of each core, the average permeability value after ageing was taken to be 900 md for each sandpack.

Relative Permeability Calculations

From the wealth of saturation data collected for the gravity flood in each sandpack, data at specific times was selected for inclusion in the relative permeability analysis. The saturation measurements from the end of each sandpack have been excluded from the analysis (although the saturation data at the inlet end of the core was used as part of the local Darcy velocity calculation), since end-effects have a significant affect on oil displacement:

- both the inlet and outlet of the packs showed evidence of lower permeability, unrepresentative of the rest of the pack,
- towards the bottom of the pack, capillary pressure effects are significant.

The relative permeability values computed for the 208 cp oil (Sandpack 1) are shown on a log-log plot against oil saturation in Figure 5. Data is grouped, by symbol, according to the depth at which each measurement was made. Although there is some scatter, the relative permeability values are clustered around an obvious trend. Oil saturation values range from 0.16 to 0.70 for this pack (the gravity floods in the other two packs employed lower viscosity oils and therefore lower oil saturation values were attained).

The data shows a scatter of approximately a factor of 6 between the highest and lowest relative permeabilities for a given saturation. Some of the scatter may reflect the fact that an average oil permeability is being used to calculate the relative permeabilities. Local changes in permeability will be reflected in artificially low relative permeabilities in low permeability zones, and artificially high relative permeabilities in high permeability zones. In this case, the local permeability would be expected to correlate with the local porosity, for which there is a direct measure from the 100% gas calibration scan in each sandpack. Attempts were made to reduce the scatter in the relative permeability data for all three

sandpacks by postulating a simple correlation linking porosity and the local permeability. This was not successful, except at a few isolated positions with relatively very low porosity. In the section on simulation of the corefloods it will be shown that in the presence of capillary pressure, the relative permeability computed at a particular depth station is not only sensitive to the local permeability, but also to the permeability in the neighbourhood of the spatial position at which it is calculated.

Since an average sandpack permeability has been assumed in the computation of relative permeabilities, the relative permeability values plotted in Figure 5 should really be considered as “effective relative permeabilities” based on the assumption of the sandpack having permeability of 0.9 Darcy.

The relative permeabilities calculated from the saturation profiles for the 23.5 cp oil (Sandpack 3) are plotted in Figure 6. For two of the depth stations, the computed relative permeability values are significantly lower than elsewhere in the sandpack. These depths (50.5 and 51.0 cm from the top of the pack) correspond to locations at which the porosity is significantly lower than elsewhere, and so are likely to correspond to a lower permeability at these positions compared to the core average.

The relative permeabilities calculated from the saturation profiles for the 2.7 cp oil (Sandpack 2) are plotted in Figure 7. As in Sandpack 3, some relative permeability data lies significantly below the rest of the data. These low values correspond to locations of low porosity - i.e. depths 40.0 and 40.5 cm from the top of the pack.

The relative permeability values computed for all three sandpacks are combined in Figure 8 which clearly shows that, in spite of the different oil viscosities employed in each flood, the relative permeabilities are all clumped around a single trend-line. All of this data has been fitted to a standard Corey relative permeability equation:

$$k_{ro} = K_{ro}^o \left(\frac{S_o - S_{org}}{1 - S_{wc} - S_{org}} \right)^n, \quad (3)$$

where K_{ro}^o is the Corey coefficient, n the Corey exponent, S_{org} is the residual oil saturation to gas flooding and S_{wc} is the connate water saturation.

The best fit through the computed relative permeability data for all three sandpacks is found to be:

$$k_{ro} = 3.55 \left(\frac{S_o - 0.035}{1 - S_{wc} - 0.035} \right)^{2.85}, \quad (4)$$

where the average connate water saturation, S_{wc} , for all three sandpacks is 0.086.

The sandpack oil relative permeabilities have also been compared with relative permeabilities determined in previous studies using Clashach cores. Figure 9 includes the results of experiments in water-wet and intermediate wet Clashach sandstone [3]. Although the relative permeabilities were very similar for the different Clashach cores (from which it was concluded [3] that the change in rock wettability affected absolute permeability rather than oil relative permeability), the relative permeabilities computed for the three sandpacks

are significantly higher. This would indicate that the very different pore structure of consolidated Clashach core and a sandpack affects both absolute permeability and oil relative permeability.

SIMULATIONS OF GRAVITY DRAINAGE

Using the black oil option in *techSIM*, a number of gas/oil gravity drainage experiments have been simulated, with the aim of understanding the temporary, local hold-up of oil observed in the saturation measurements made using 208 cp oil.

Two types of heterogeneous model have been run:

- without capillary pressure
- with capillary pressure that is independent of the local value of permeability.

Previous studies of the effect of reservoir heterogeneity on gravity drainage [4], suggest that where capillary pressure scales with permeability, less hold-up of oil is found above low permeability zones, with the results being closer to the local hold-up due to permeability effects alone. The cases run are therefore expected to bracket the range of possible behaviour. Earlier it was noted that attempts to correlate local porosity with local differences in saturation were not successful. This would be expected if higher local oil saturations occur in high permeability regions above low permeability zones, as a result of capillary pressure effects. For the limited range of permeabilities considered, this effect will be most evident in simulation models with capillary pressure that is independent of permeability.

Capillary Pressures

The experimental oil saturations plotted in Figures 2, 3, and 4 exhibit capillary end effects, causing a hold-up of oil towards the base of the sandpicks. If gravity drainage were to continue until equilibrium were achieved throughout the core, then the capillary pressure, p_c , would be given by:

$$p_c(S_o(z)) = (L - z)g \Delta\rho, \quad (5)$$

where $S_o(z)$ is the oil saturation distribution, and distance z is measured downwards from the inlet of the sandpack (assuming p_c is zero at the sandpack outlet). Since Sandpack 2 used the lowest viscosity oil the final saturations in the gas flood will be closest to the capillary-gravity equilibrium defined by (5), and so this has been used as the basis for the capillary pressure function used in the simulations.

Simulations of Simple Heterogeneities

In order to help understand the role of permeability variations and capillary pressures in the gravity drainage experiments, simulations have been performed using an idealised pack with a uniform permeability (900 md) apart from two narrow tight zones (with permeability 225 md). Equation (4) has been used to define the relative permeability in the simulation.

Figure 10 illustrates the simulated oil saturations, assuming zero capillary pressure. The two tight zones give rise to localised “hold-up” in the computed oil saturation profiles. The

oil saturation data was used to compute relative permeabilities, using the same methodology used for analysing experimental oil saturations, and the results shown in Figure 11. Most of the computed relative permeability values match the defined relative permeabilities. However, at the two depths corresponding to the lower permeability zones, computed relative permeabilities drop below the trend-line. This is because the computational procedure has assumed a uniform permeability, giving a local permeability which is 4× higher than the real permeability value at these depths.

Figures 12 and 13 illustrate the oil saturations and computed relative permeabilities based on a gravity drainage simulation in which non-zero capillary pressure is assumed (but where capillary pressure is independent of local porosity and permeability). Where permeability is locally low, the capillary pressure reduces the oil saturation hold-up and also raises the hold-up upstream of the tight zone (compare the “high points” in Figures 10 and 12). This smoothing of the oil saturation profile can be explained mathematically by differentiating equation (5):

$$g \cdot \Delta\rho = \frac{d}{dz} p_c(S_o(z)) = \frac{dp_c}{dS_o} \frac{\partial S_o}{\partial z}. \quad (6)$$

The greater the slope $\frac{dp_c}{dS_o}$, the smaller any local fluctuations in S_o will be.

Most of the relative permeabilities computed from the oil saturation profiles again match the defined relative permeabilities (Figure 13), but with non-zero capillary pressure the computed relative permeability values are not only reduced at the tight permeability zones, but also at depth stations near to these tight zones. This indicates that the scatter of relative permeability datum points observed in the analysis of experimental data is caused not only by permeability heterogeneity, but also by capillary pressures. Even if an accurate permeability distribution were available for a sandpack, it would not be possible to remove the scatter by scaling each computed relative permeability value according to the local permeability.

Simulations of Heterogeneous Packs

For simulation purposes, a pack with the local permeability varying along its entire length has been defined. The permeability fluctuates between 250 and 1931 md, with a profile designed to give computed oil saturations similar to those observed in the gravity drainage experiments using the 208 cp oil. The mean permeability is 900 md, as in the actual sandpacks.

In the absence of capillary pressure, gravity drainage is simulated to give the oil saturations shown in Figure 14 for conditions equivalent to Sandpack 1. When capillary pressure is included, the degree of “noise” in the oil saturation profiles is reduced, see Figure 15. The fact that the degree of local hold-up of oil was greater in the laboratory coreflood than in the simulation could indicate that:

- the simulated gravity drainage experiments overestimate the capillary pressure (since capillary pressure has the effect of smoothing any spatial fluctuations in oil hold-up), or
- the degree of permeability heterogeneity may have been greater than assumed in the simulation, or

- the capillary pressure function may be a function of position through porosity or permeability.

When the oil saturations in Figure 15 are used to compute relative permeability values, Figure 16 is obtained. As described in the previous section, the scatter is due to the heterogeneity (the maximum local permeability is almost eight times higher than the minimum value) and is also affected by capillary pressure. Most of the computed relative permeability values lie slightly above the relative permeability curve defined in simulator input, since most of the local permeability values are higher than the mean value of 900 md. The mean permeability reflects the harmonic average of local permeability values. The arithmetic mean of local permeability values is 1117 md, so that for most of the depth stations in the simulated pack, the local permeability is underestimated, leading to a computed relative permeability value which is higher than the average.

A best fit line through the relative permeability values in Figure 16 would not be identical to the relative permeability defined in the simulator input. This indicates that the relative permeabilities computed from analysis of oil saturations in a gas/oil gravity drainage represent effective relative permeabilities, although in this case they are very close to the actual relative permeabilities.

The simulation model for Sandpack 1 has been modified to represent an oil of viscosity 2.7 cp, and a drainage rate of 2 ml/hr, thus matching the conditions in the Sandpack 2 gravity drainage experiment. The simulated oil saturations are plotted in Figure 17. Just as in the experimental oil saturations (Figure 2), far less localised oil hold-up is observed than with the more viscous oil. Now that the role of capillary pressures in gravity drainage is understood, a reason can be given for the relative lack of oil hold-up observed with the low viscosity oil. In the lower viscosity oil experiments (Sandpacks 2 and 3), the gas saturations reach much higher values than was the case in the 208 cp experiments. The capillary pressure gradient increases with gas saturation, and since capillary pressure acts to smooth out spatial variations in oil saturation, it follows that less localised hold-up of oil would be associated with heterogeneities in Sandpacks 2 and 3 compared to Sandpack 1.

ESTIMATING RESIDUAL OIL SATURATIONS DURING GAS FLOODING

In order to assess the impact which the computed relative permeability values could be expected to have in practical reservoir drainage applications, a series of Buckley-Leverett calculations have been performed. These 1-dimensional vertical displacement calculations estimate the local residual oil saturation at various reservoir flow rates for a range of oil viscosities. The calculations are representative of gravity stable gas displacement, and assume no coning or capillary pressure effects.

In a reservoir with vertical permeability of 5 Darcy, the breakthrough results plotted in Figure 18 are obtained. These calculations assume:

μ_g	0.025 cp
$\Delta\rho$	800 kg/m ³
k_{rg}	=0.5(S_g) ² (a typical Corey equation for gas relative permeability)
ϕ	0.35
S_{wc}	0.10

For oil viscosities below ~100 cp the microscopic sweep efficiency obtained with gas flooding can be seen to be gravity dominated for displacement rates of ~10 ft/month and below. Note that the velocities represented on the Buckley-Leverett plots are *interstitial velocities*, given by the Darcy velocity divided by porosity. In an efficient displacement the interstitial velocity is an approximate measure of the speed of the gas front. Under appropriate conditions, effective residual oil saturations of ~10% may be obtained for oils of 100 cp viscosity.

A similar calculation has been performed for a reservoir with 1000 md vertical permeability, see Figure 18, representative of a 5000 md reservoir with a $k_v:k_h$ ratio of 0.2. For gravity dominated conditions the recovery is equivalent to that shown for the 5000 md vertical permeability, but at rates reduced by a factor of 5 [5].

CONCLUSIONS

Analysis of pressure drop data during conditioning allowed regions of low oil permeability at the inlet and outlet ends of the sandpacks to be excluded from the subsequent analysis.

Oil relative permeabilities have been calculated from the in-situ saturation data for the three sandpacks. The relative permeabilities lie on the same curve, showing that oil relative permeabilities are independent of viscosity over the range 2 to 200 cp in these sandpacks.

Comparison of the sandpack relative permeabilities with data obtained from consolidated Clashach sandstone, shows that the relative permeabilities in the sandpacks are approximately a factor of 300 higher over the saturation range considered. Gravity drainage in high permeability unconsolidated reservoirs, even with viscous oils, is therefore potentially a very efficient displacement technique.

The oil saturations measured during gas/oil gravity drainage experiments with 208 cp oil showed significant temporary hold-up of oil. The degree of hold-up was much lower for the experiments using less viscous oils. Simulations of the gravity drainage experiments demonstrate that the local hold-up is probably a consequence of the heterogeneity of the pack, and that capillary pressures act to reduce the local hold-up. The higher gas saturations achieved with the less viscous oils correspond to higher capillary pressures, giving much smoother oil saturation profiles.

One dimensional solutions for vertical displacement of oil by gas have been constructed and the effective residual oil saturation at breakthrough determined for a wide range of viscosities (1 cp to 1000 cp) and frontal advance rates (including typical reservoir rates) for

vertical permeabilities of 1000 and 5000 md. Under appropriate conditions, effective residual oil saturations of ~10% may be obtained for oils of 100 cp viscosity.

NOMENCLATURE

A	pack cross-sectional area
K	permeability
$k_b(x)$	permeability of displacing phase at position x from core inlet in local permeability calculation
$k_i(x)$	permeability of phase initially present at position x from core inlet in local permeability calculation
K_{ro}^0	Corey coefficient
k_{rg}	gas relative permeability
k_{ro}	oil relative permeability
L	pack length
n	Corey exponent
p_c	capillary pressure
Q	injection rate
S_g	gas saturation
S_o	oil saturation
S_{org}	residual oil saturation to gas flooding
S_{wc}	connate water saturation
t	time
W	total volume of injected fluid
z	depth
Δp	pressure drop
$\Delta \rho$	$\rho_{oil} - \rho_{gas}$, where ρ =density
μ_b	viscosity of displacing phase in local permeability calculation
μ_i	viscosity of phase initially present in local permeability calculation
μ_g	gas viscosity
ϕ	porosity

ACKNOWLEDGEMENT

This work was supported by the UK Department of Trade and Industry as part of its IOR studies at AEA Technology. The DTI's permission to publish is gratefully acknowledged.

REFERENCES

1. Aldrich Catalogue Handbook of Fine Chemicals 1996-7, p882
2. Relative Permeabilities for Gravity Stabilised Gas Injection, S G Goodyear and P I R Jones, 7th European Symposium on Improved Oil Recovery, Moscow, Russia October 1993
3. Gravity Drainage During Gas Injection, P Naylor, N C Sargent, A J Crossbie, A P Tilsed and S G Goodyear, Petroleum Geoscience, Vol 2, 1996, pp.69-74.
4. L J Roberts, A. W. Peacock, J. P. Taggart. "The Effect of Reservoir Heterogeneity on the Gravity Drainage of Oil with Immiscible Gas Injection", 5th European Symposium on Improved Oil Recovery, Budapest, April 1989
5. An Analysis of Composition and Rate Effects in Gravity Stabilised Gas Injection, R W S Foulser, S G Goodyear and P H Townsley, In Situ 1992, 16(4), 269-296

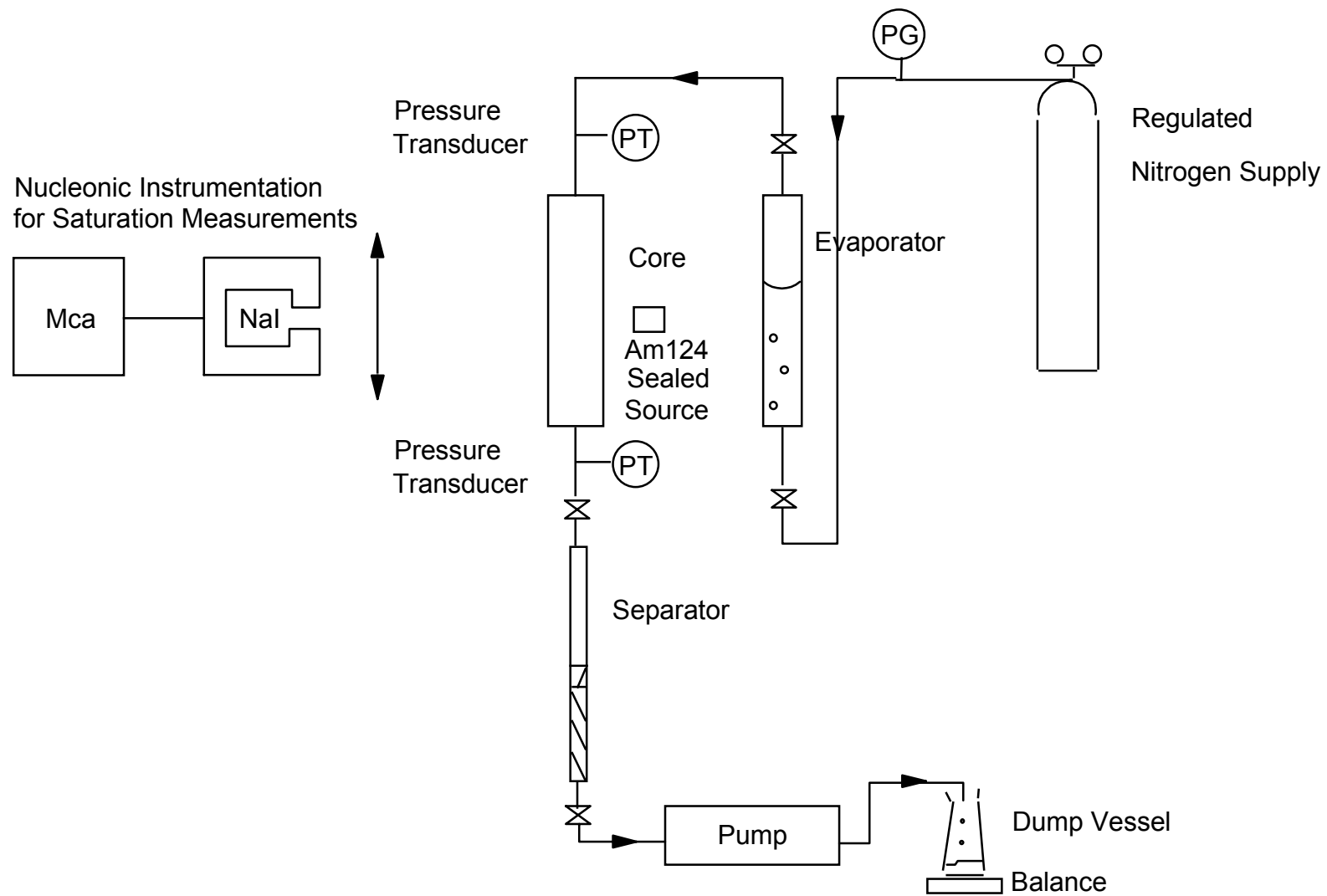


Figure 1: Schematic diagram of gas injection flow circuit

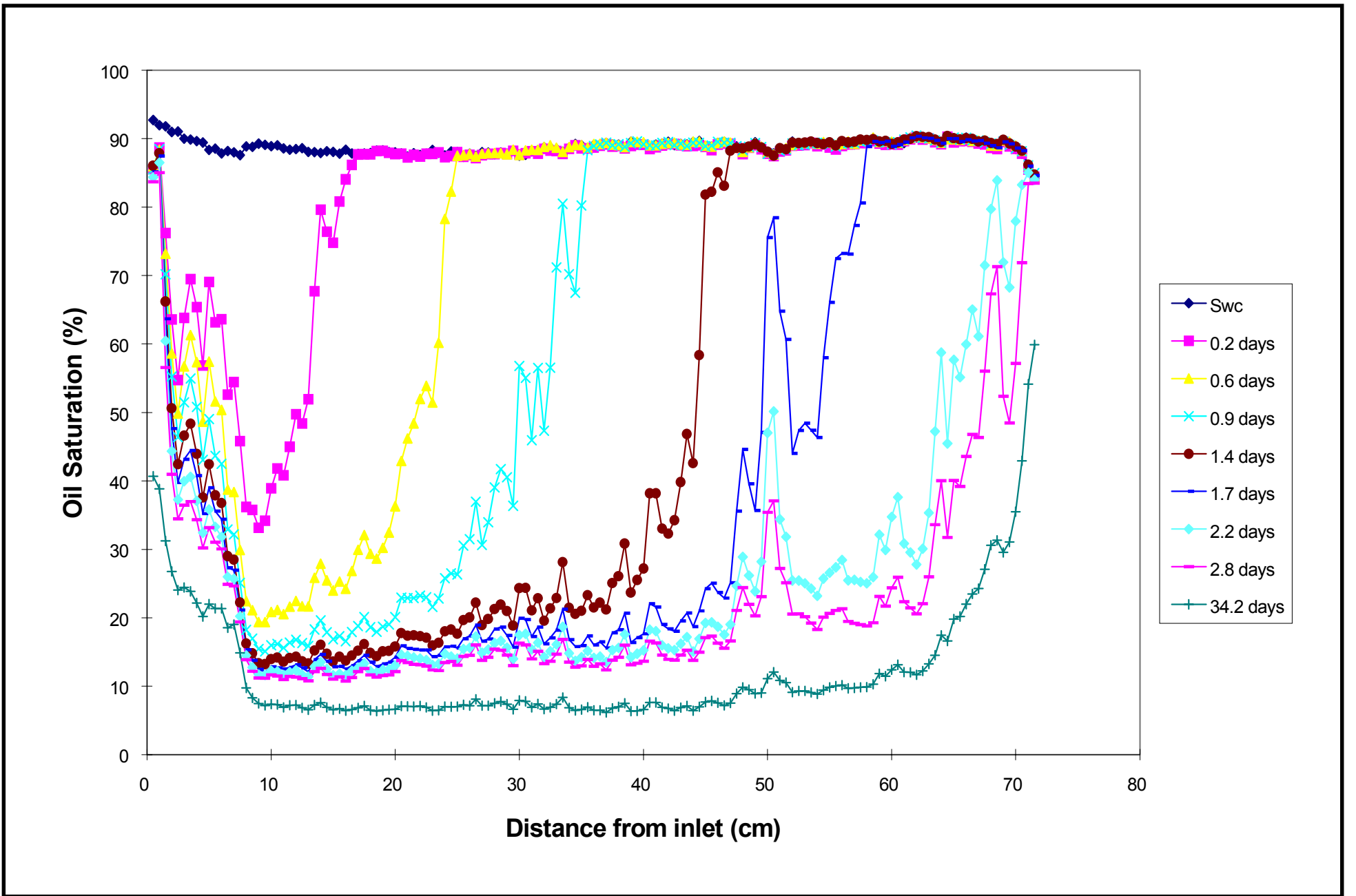


Figure 2: Oil saturation profiles for gravity drainage of 2.7 cp oil (Sandpack 2)

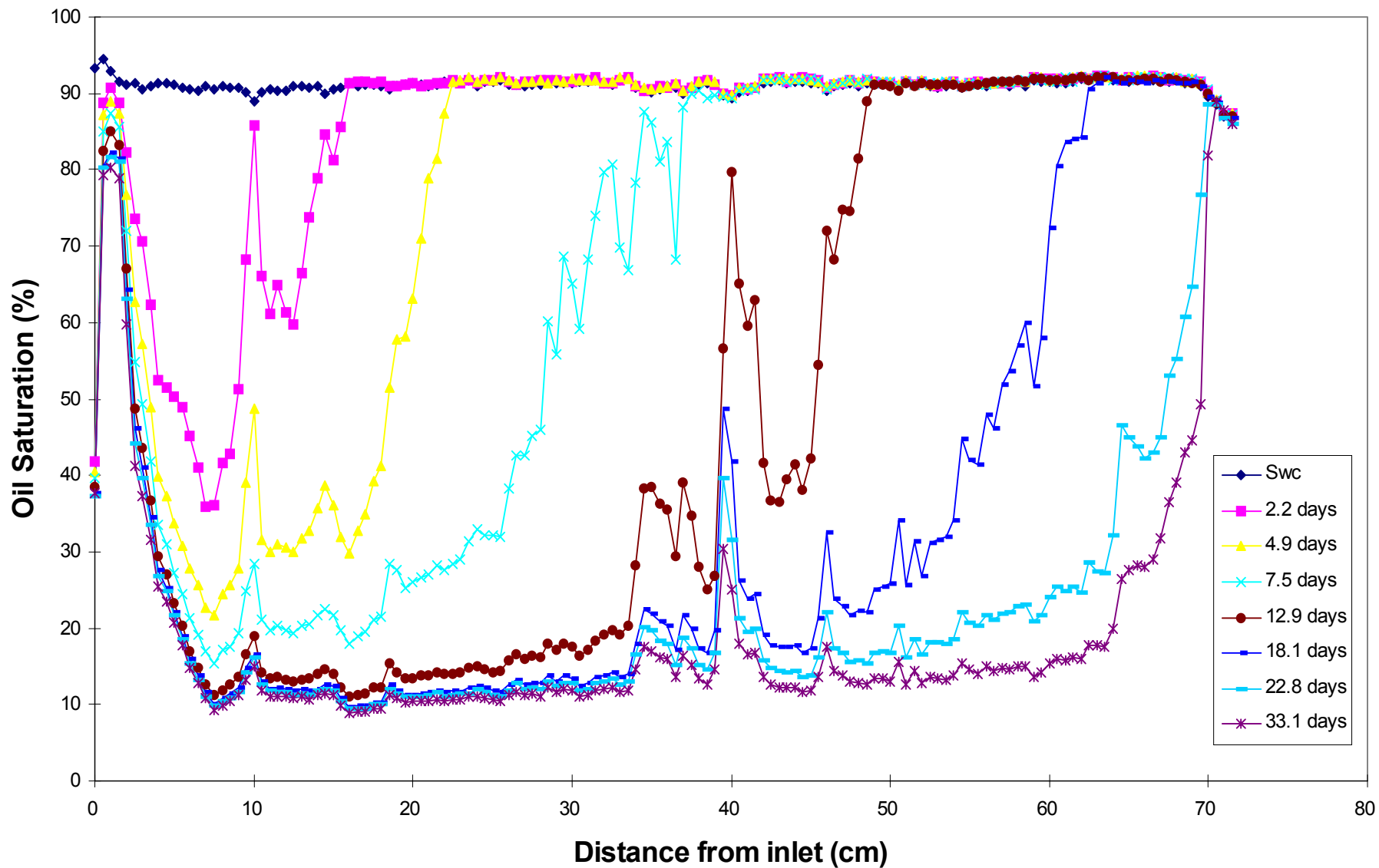


Figure 3: Oil saturation profiles for gravity drainage of 23.5 cp oil (Sandpack 3)

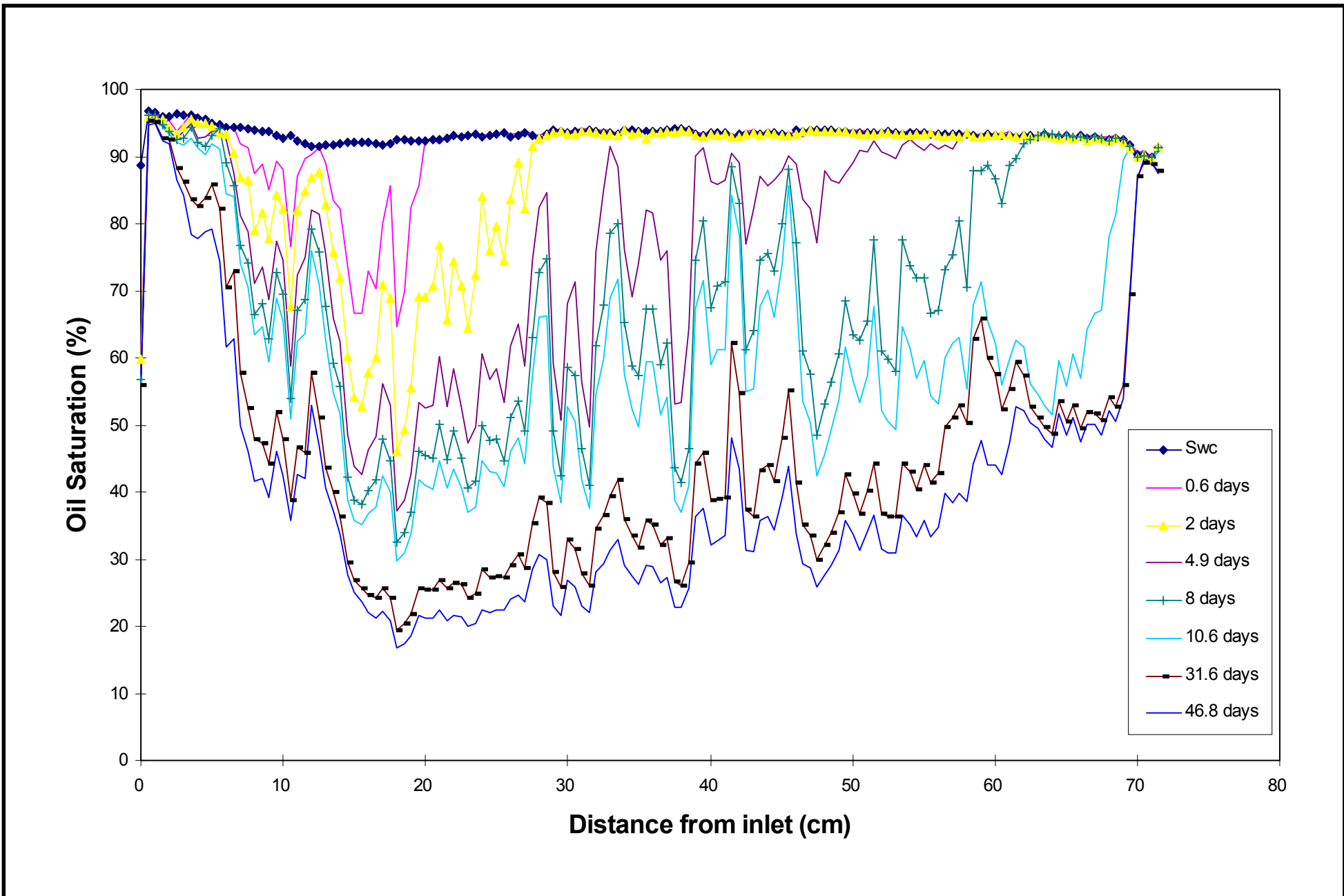


Figure 4: Oil saturation profiles for gravity drainage of 208 cp oil (Sandpack 1)

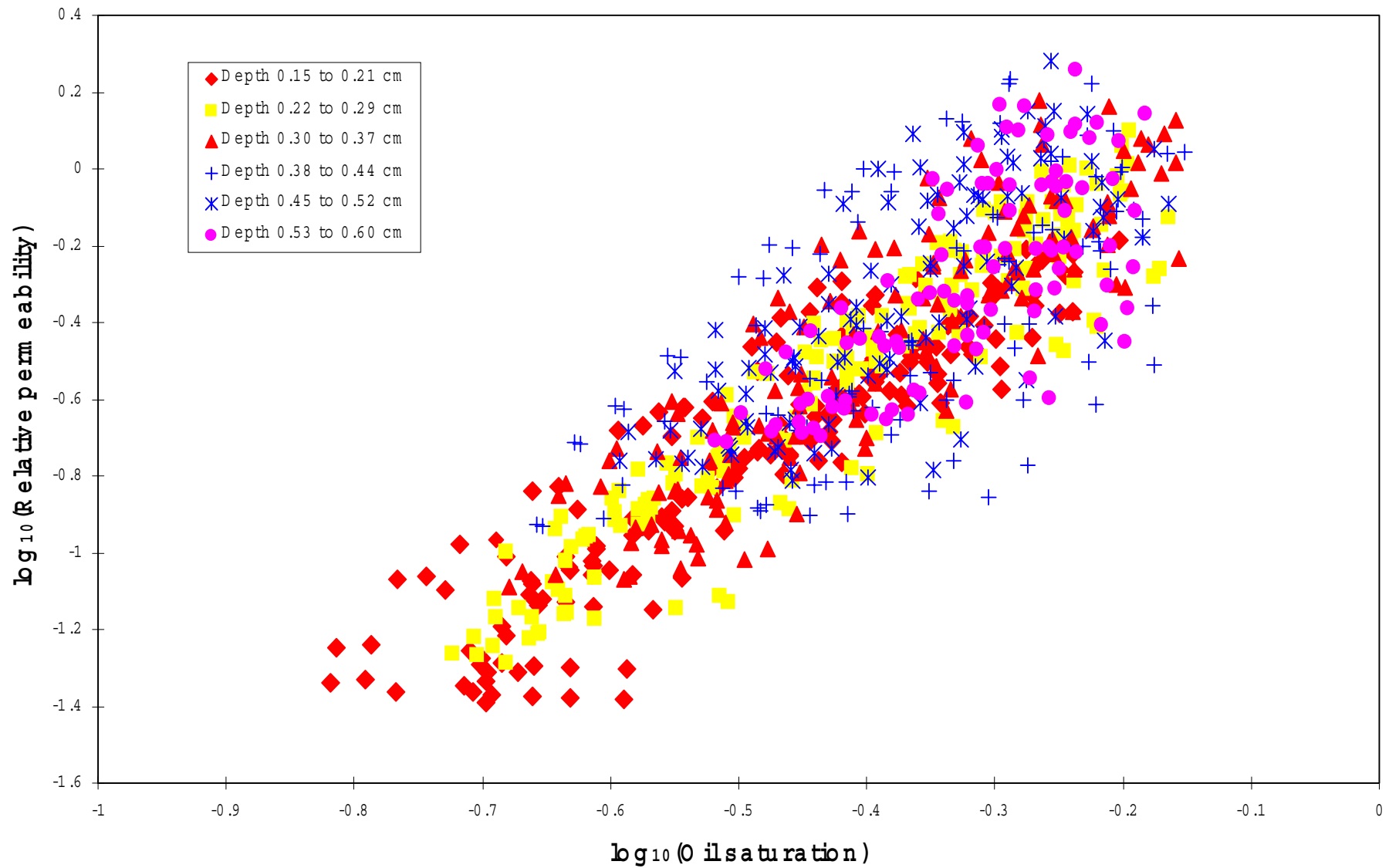


Figure 5: Oil relative permeabilities for gravity drainage of 208 cp oil (Sandpack 1)

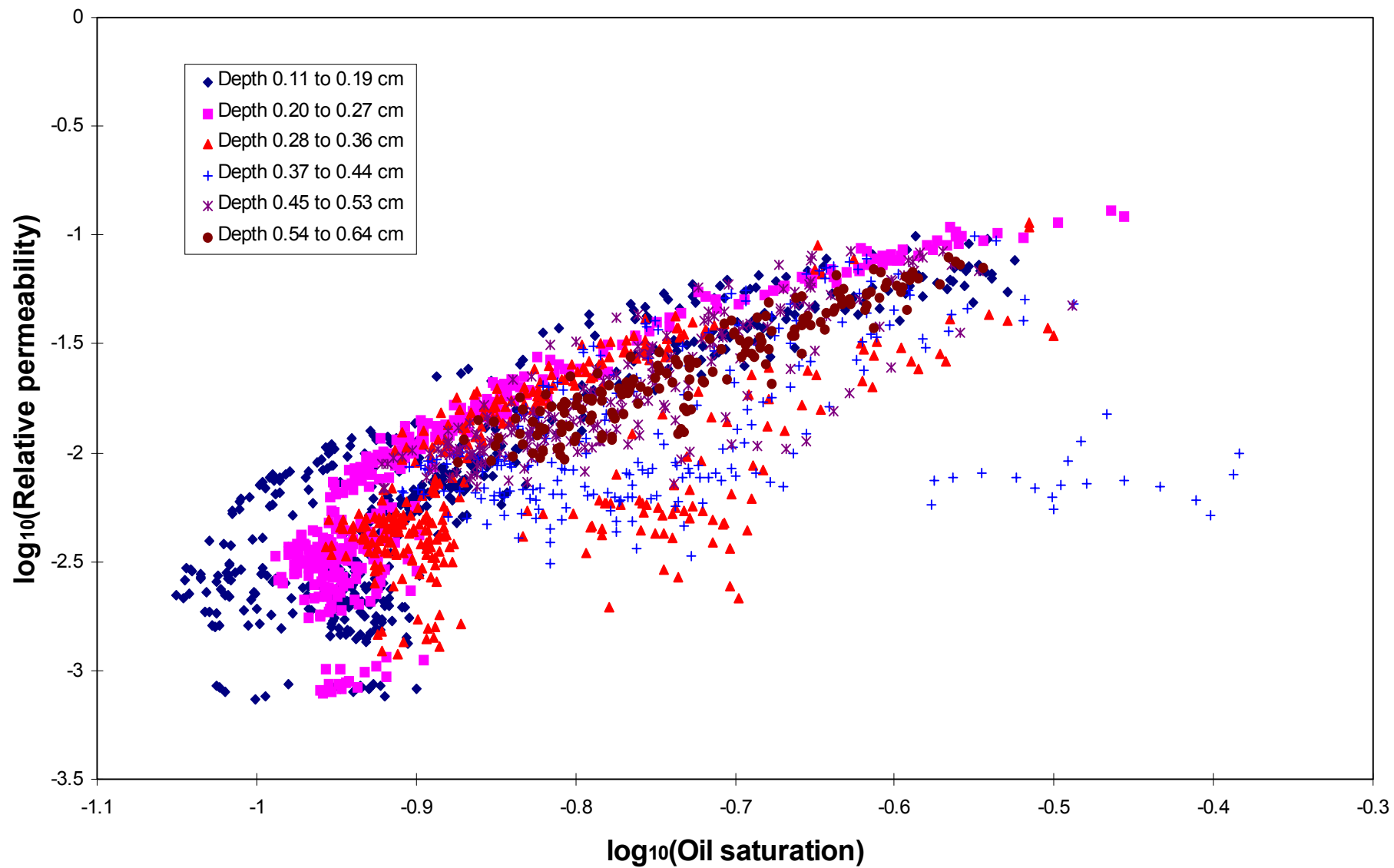


Figure 6: Oil relative permeabilities for gravity drainage of 23.5cp oil (Sandpack 3)

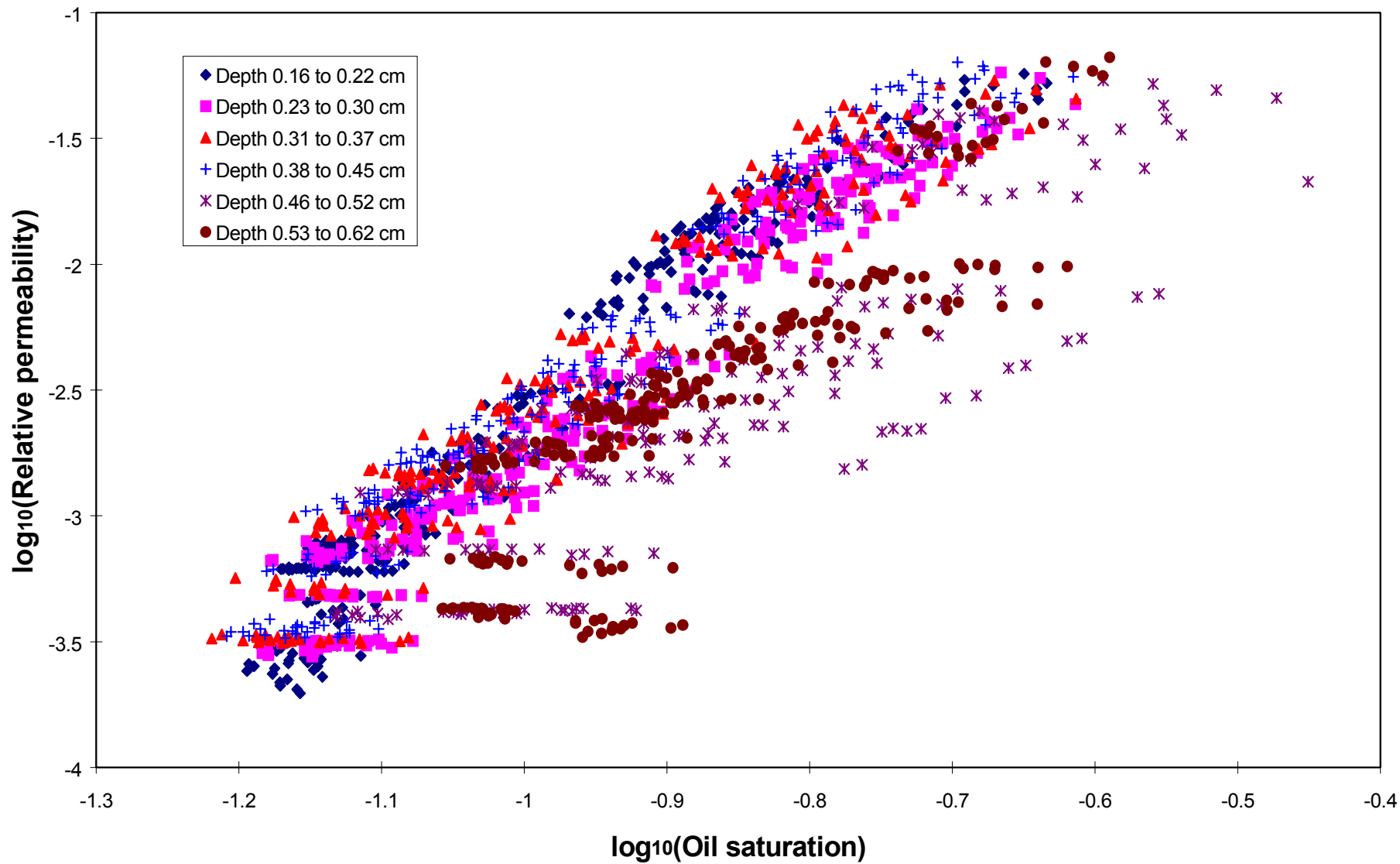


Figure 7: Oil relative permeabilities for gravity drainage of 2.7 cp oil (Sandpack 2)

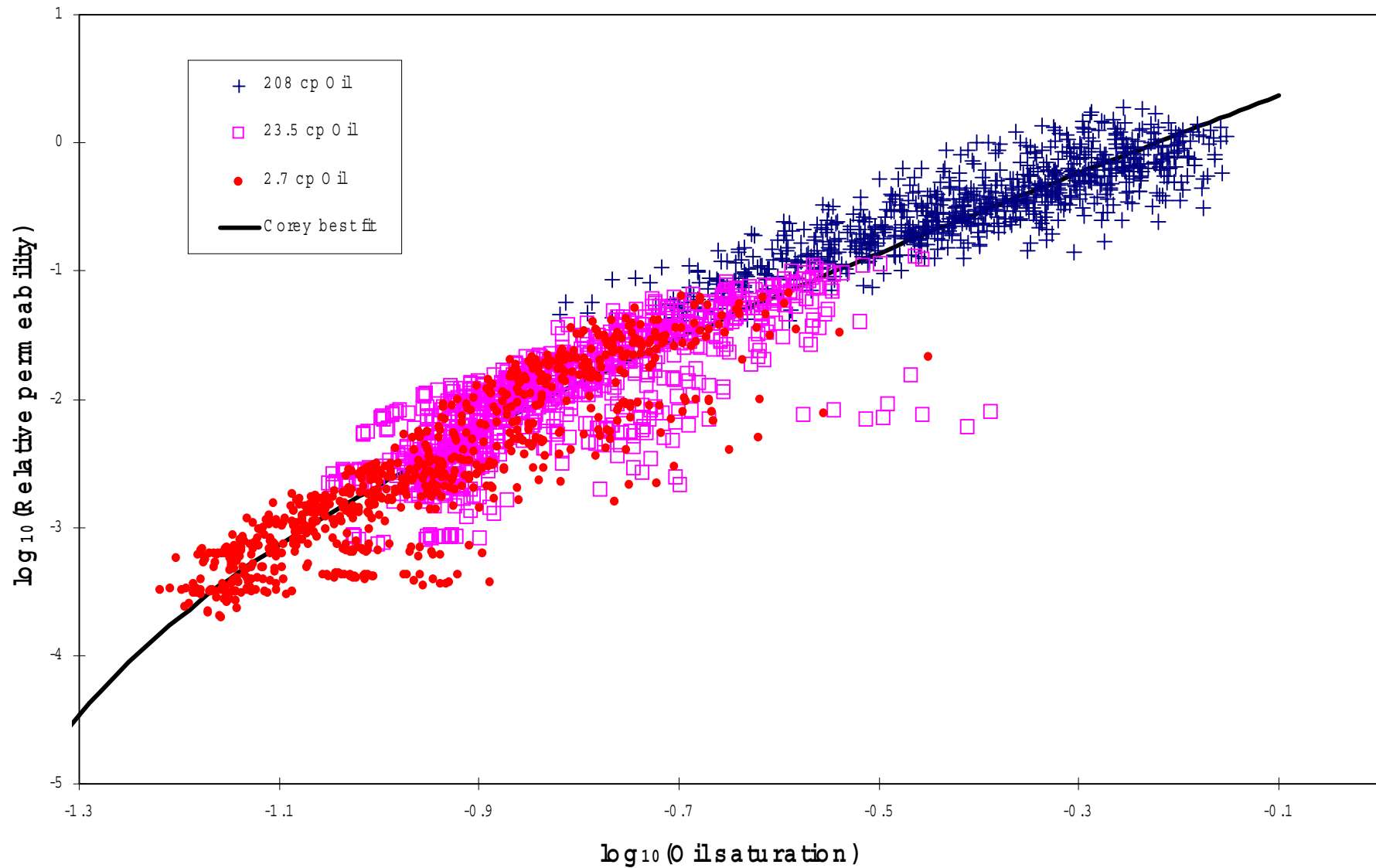


Figure 8: Comparison of relative permeabilities for different oil viscosities

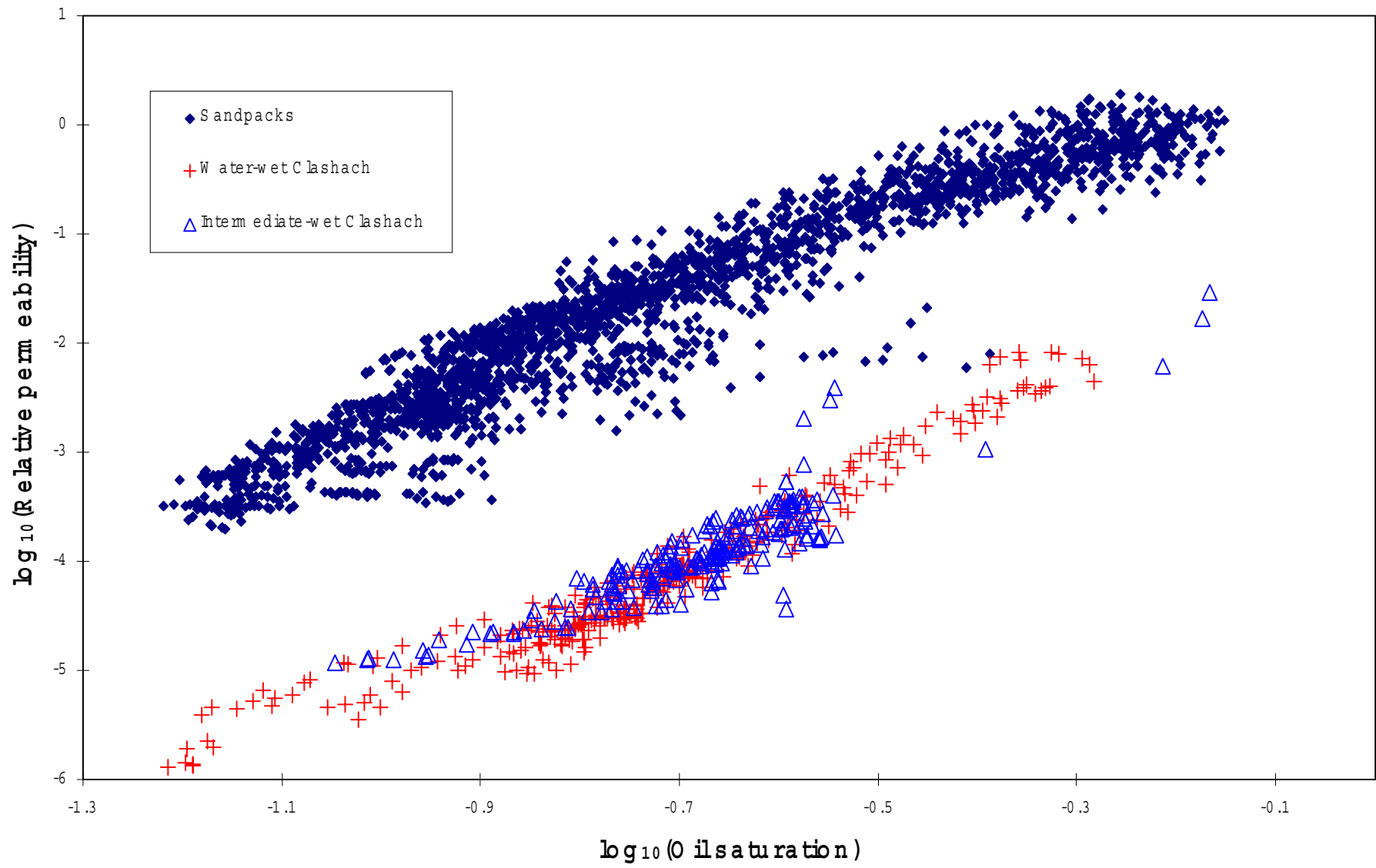


Figure 9: Comparison of relative permeabilities for Sandpacks and Clashach sandstone

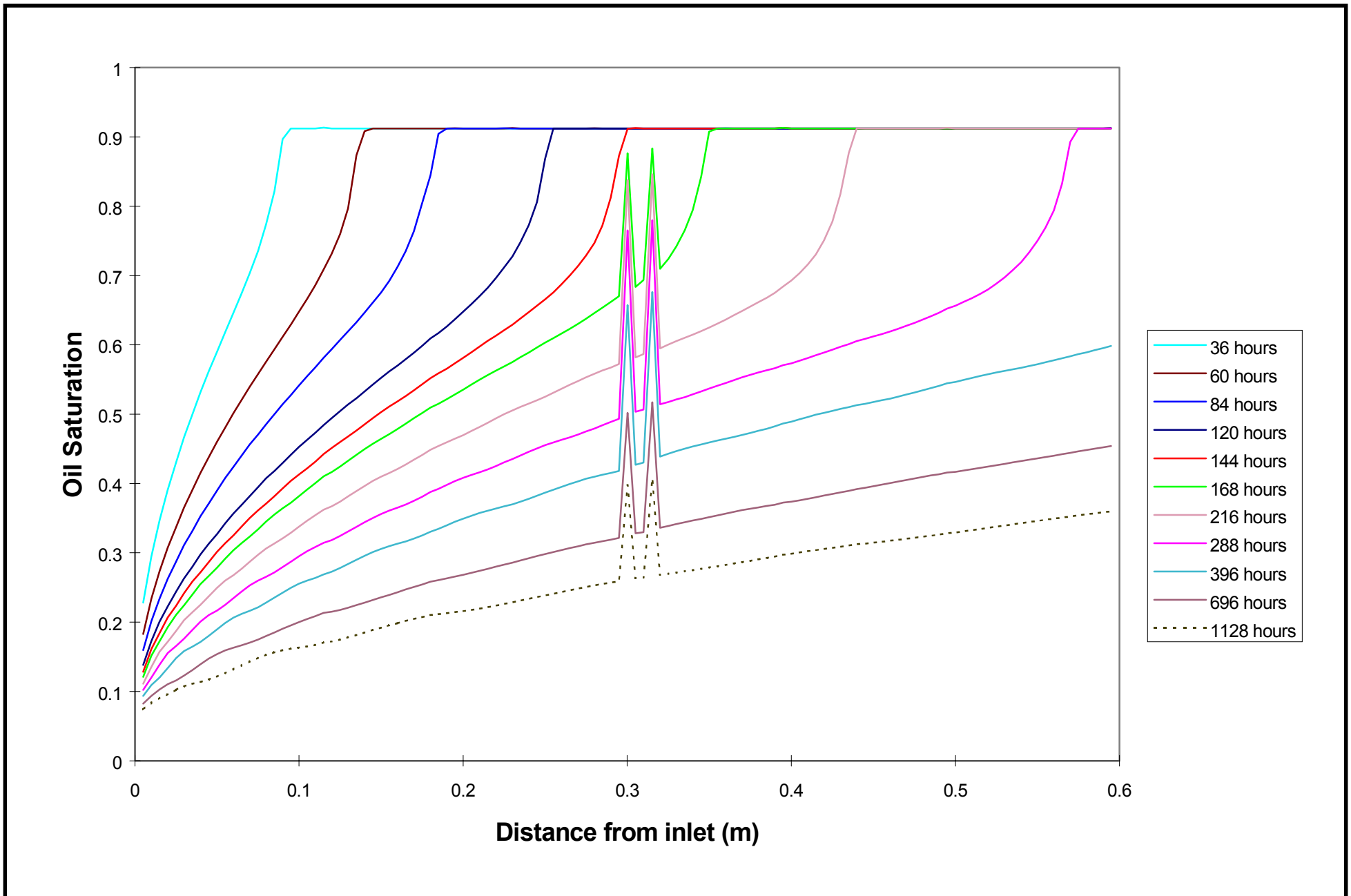


Figure 10: Simulated 208 cp oil saturation profiles for gravity drainage with simple heterogeneity

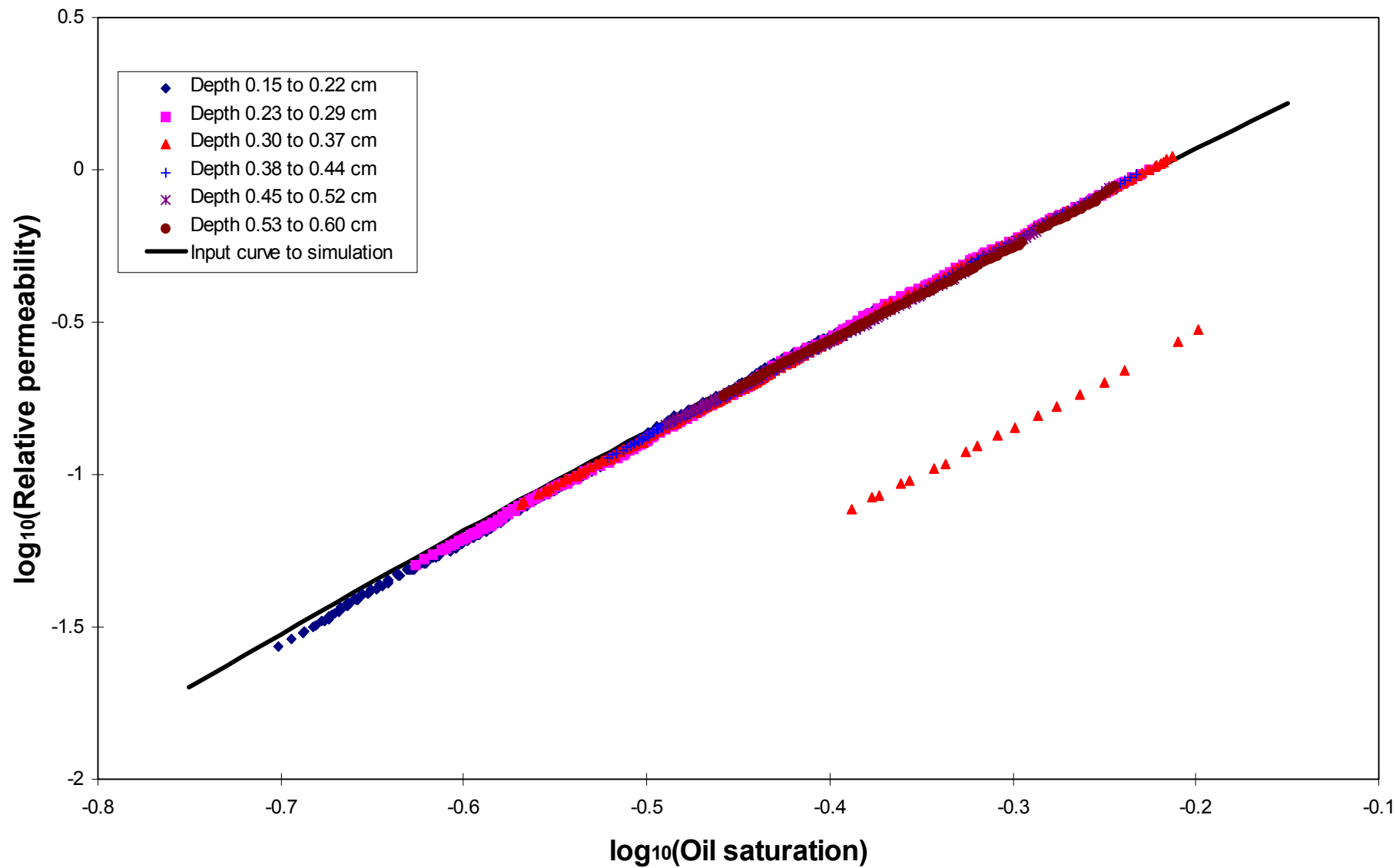


Figure 11: 208 cp oil relative permeabilities from simulated data with simple heterogeneity

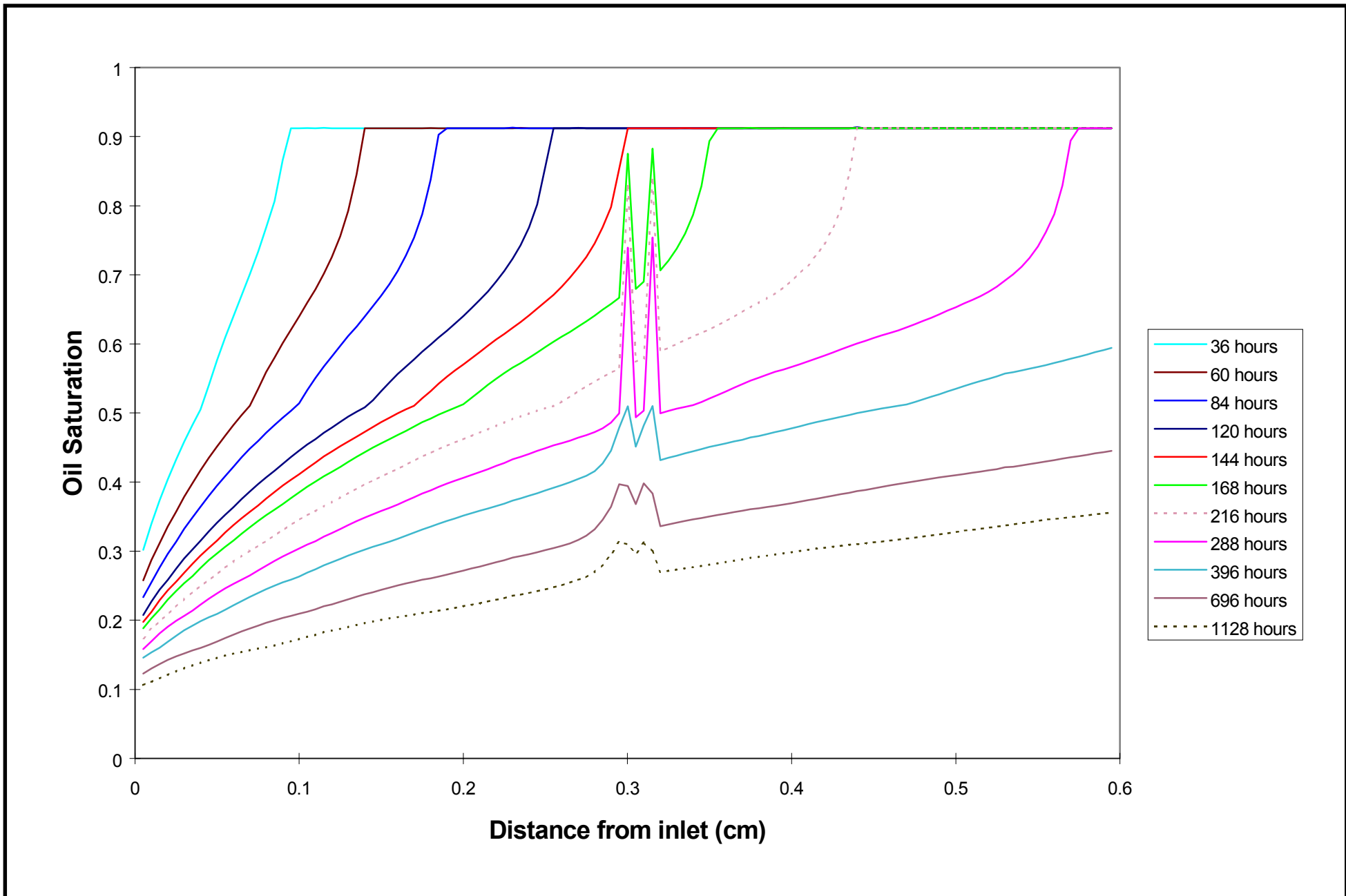


Figure 12: Simulated 208 cp oil saturation profiles for drainage with simple heterogeneity and capillary pressure

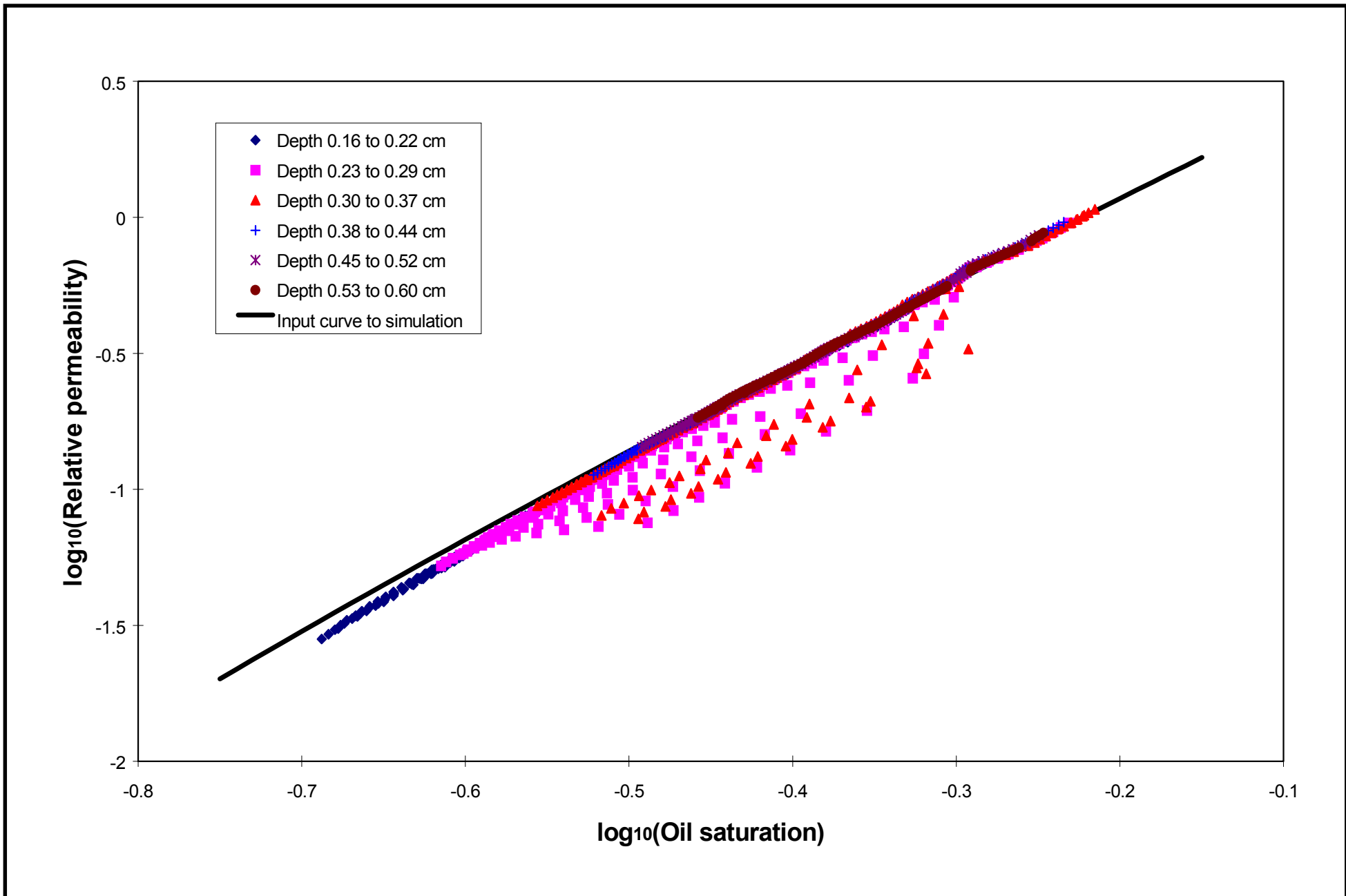


Figure 13: 208 cp oil relative permeabilities from simulated data with simple heterogeneity and capillary pressure

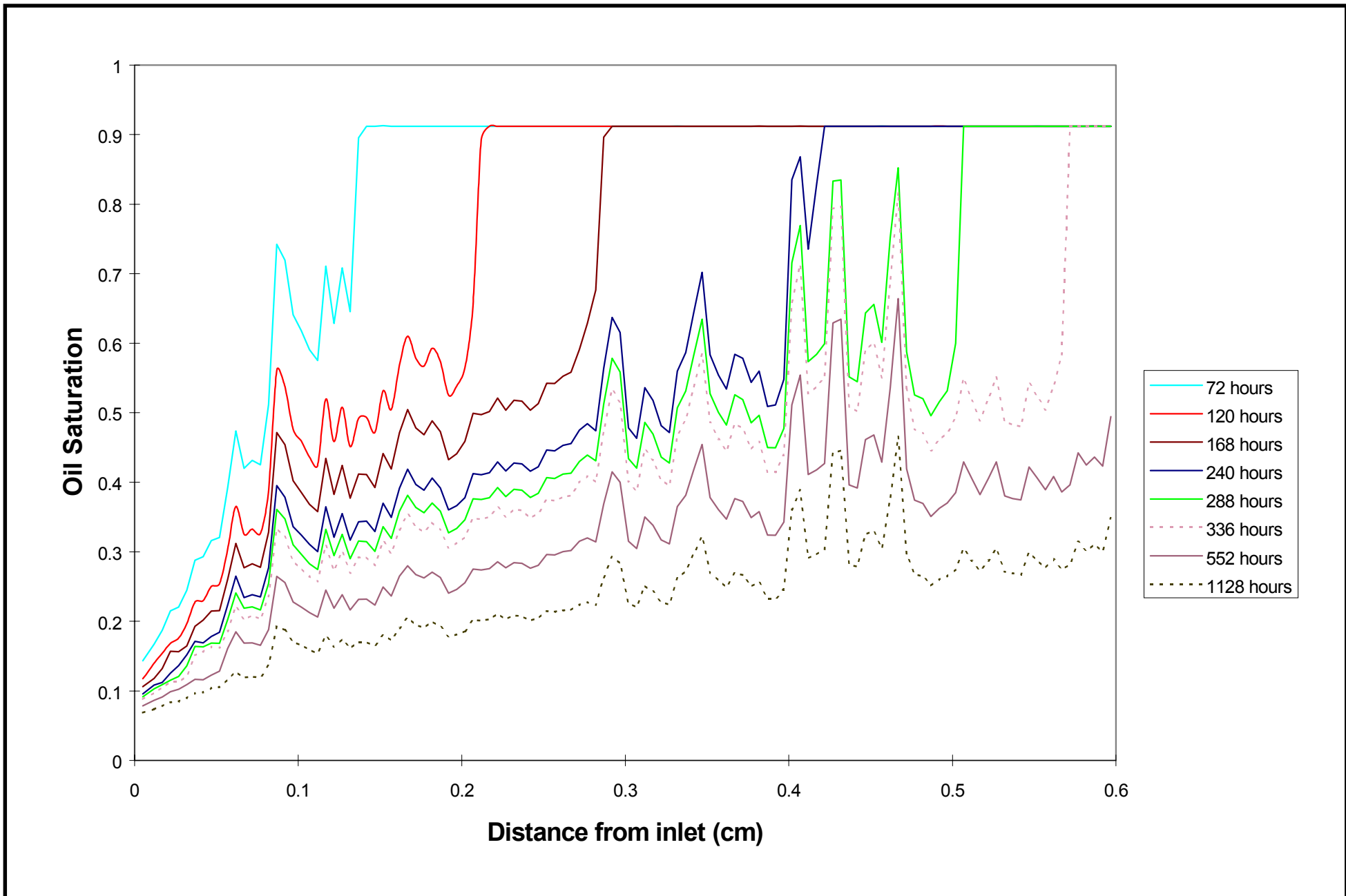


Figure 14: Simulated 208 cp oil saturation profiles for gravity drainage in heterogeneous pack

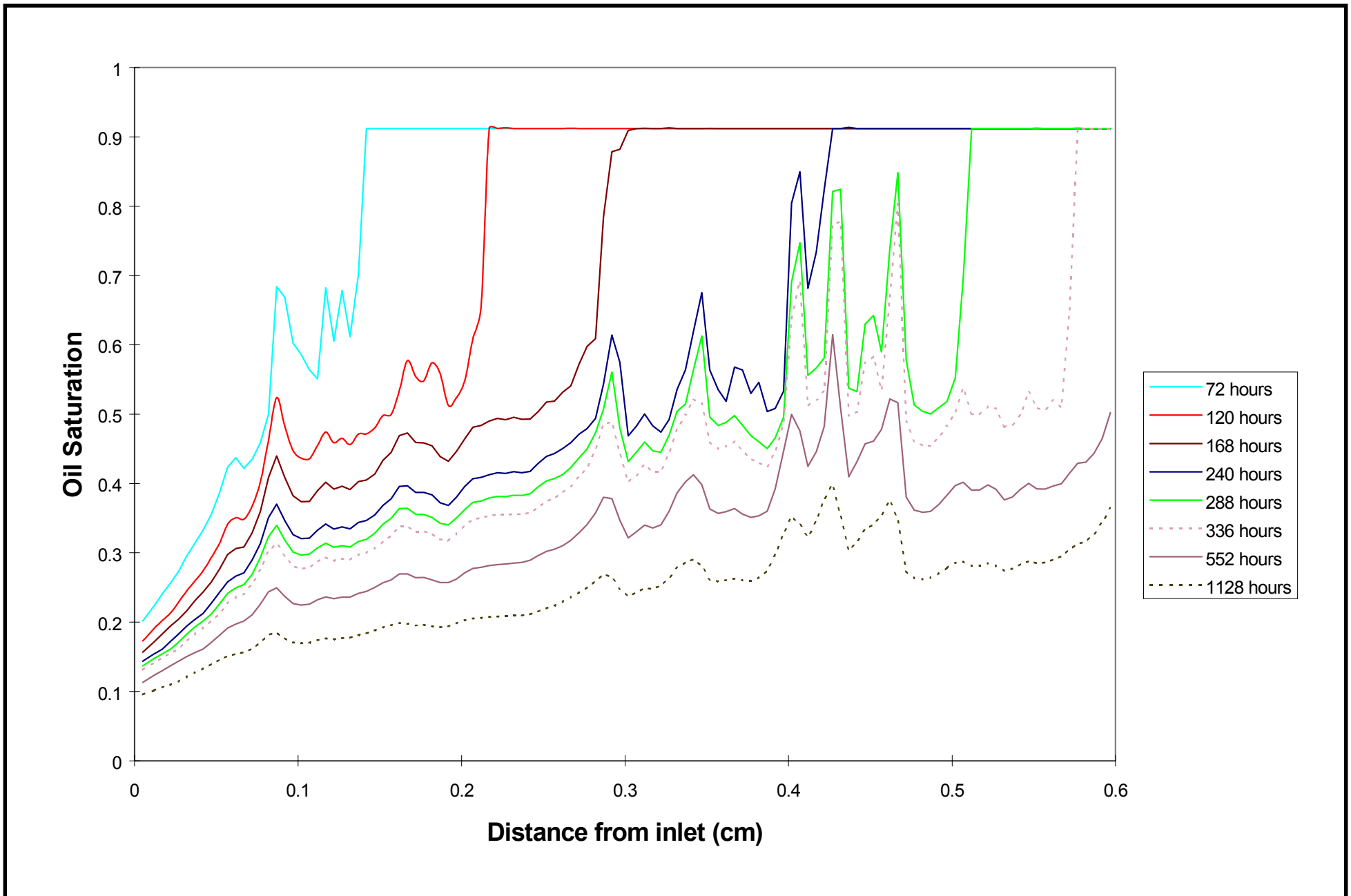


Figure 15: Simulated 208 cp oil saturation profiles for drainage in heterogeneous pack with capillary pressure

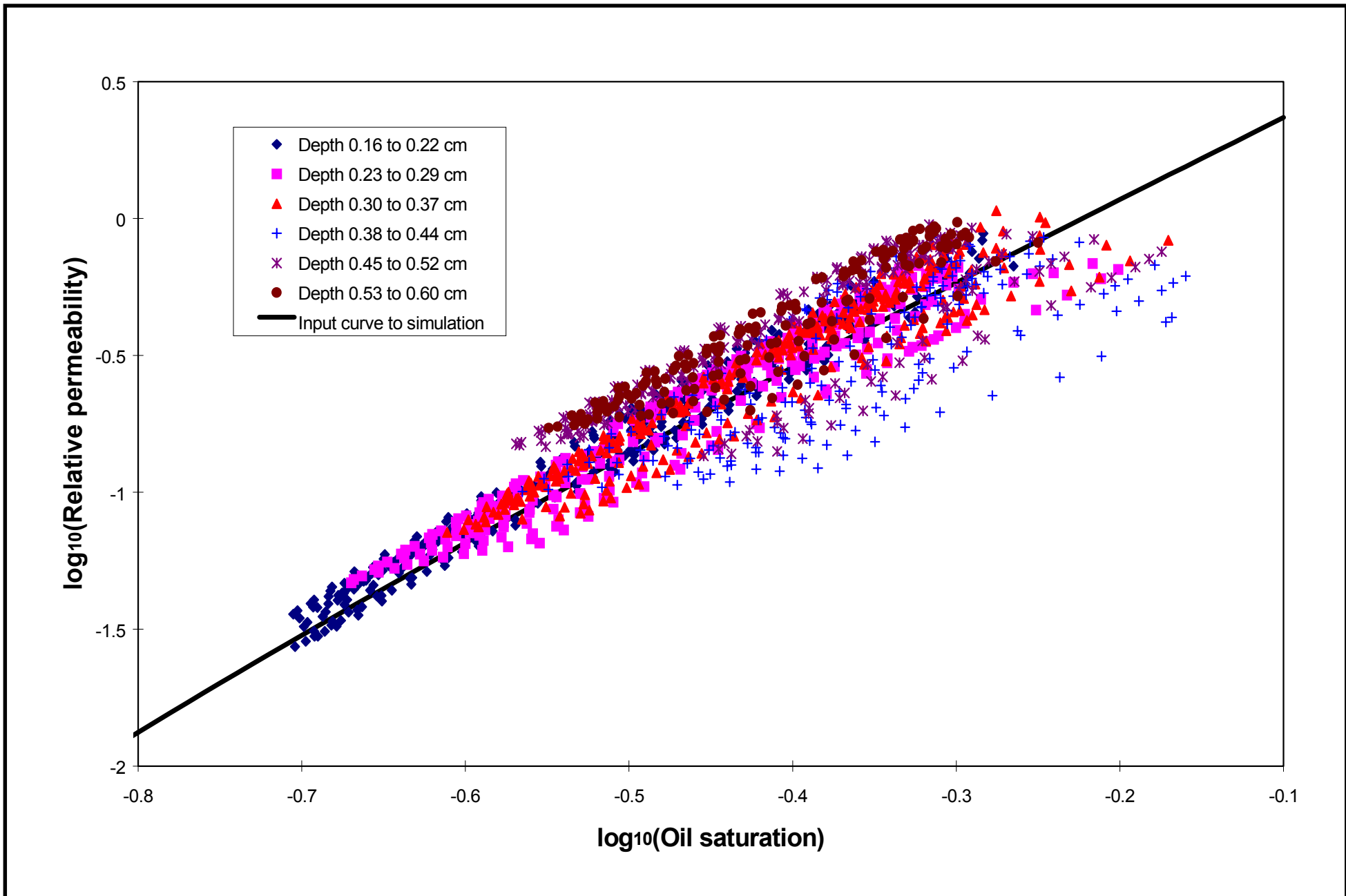


Figure 16: 208 cp oil relative permeabilities from simulated heterogeneous pack with capillary pressure

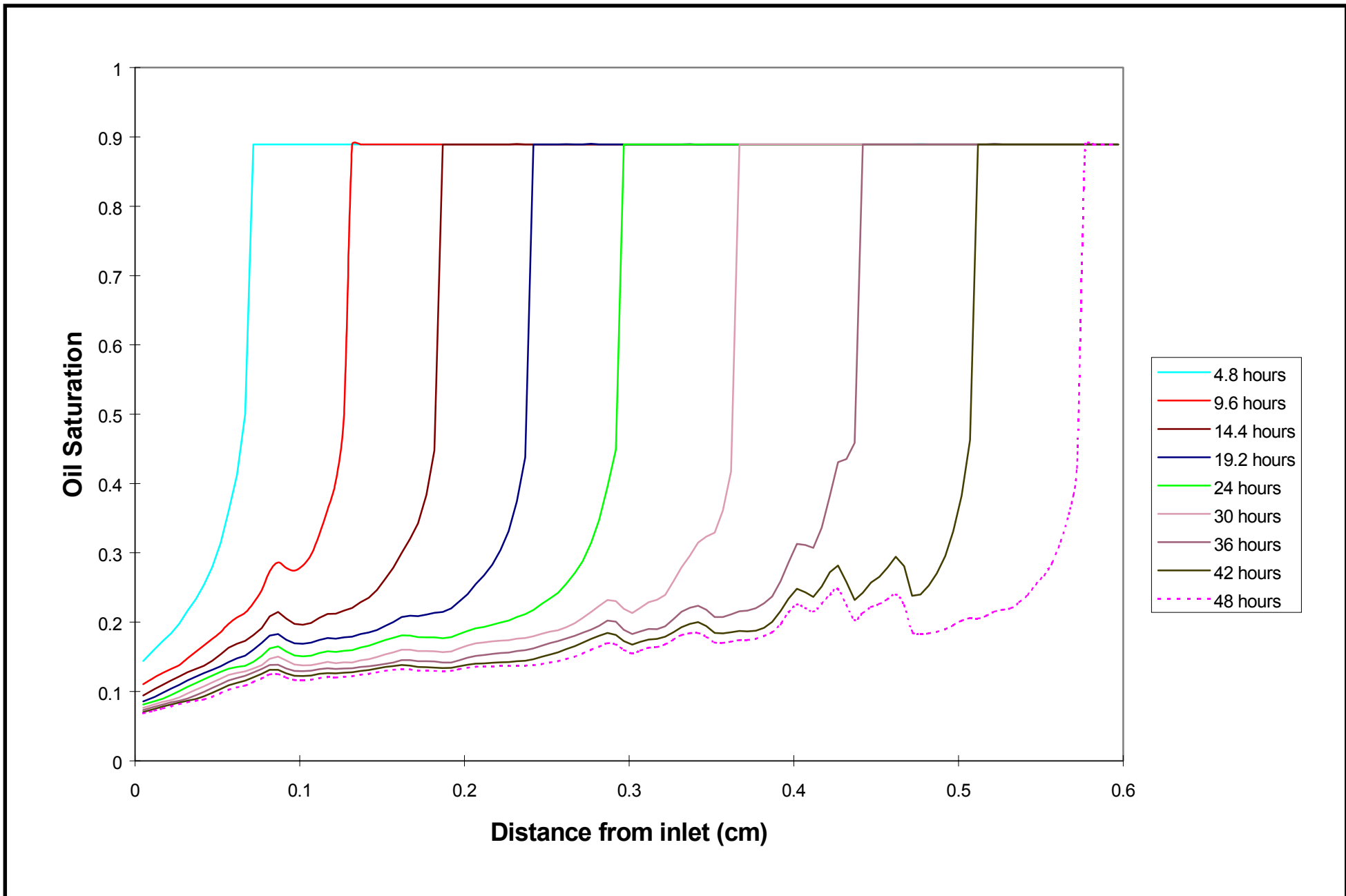


Figure 17: Simulated 2.7 cp oil saturation profiles for gravity drainage in heterogeneous pack with capillary pressure

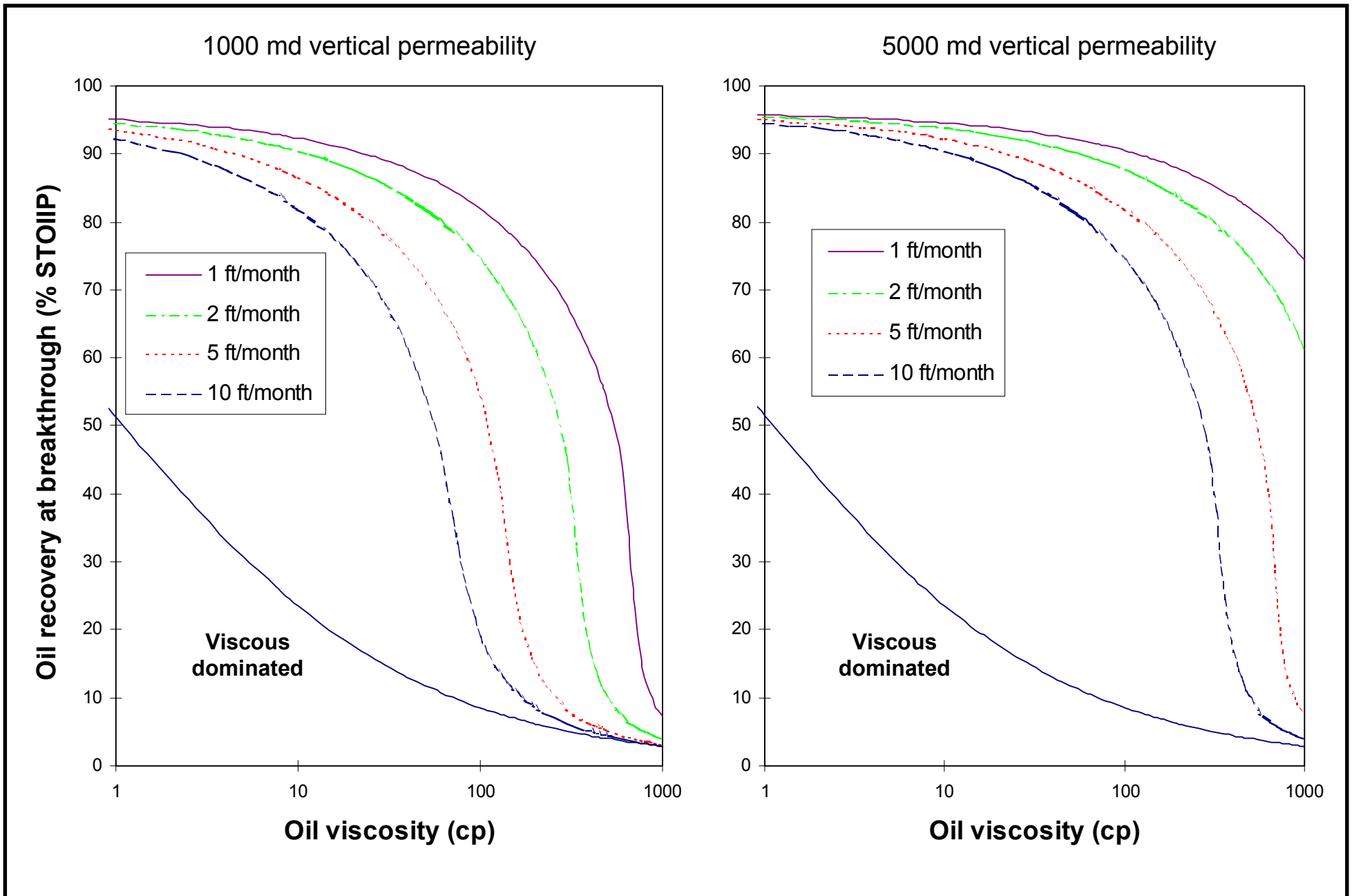


Figure 18: Oil recovery efficiency at gas breakthrough as a function of viscosity and injection rate